ANALYTIC TREATMENT OF TRACKING ERROR AND NOTES ON OPTIMAL PICK-UP DESIGN*

H. G. BAERWALD**

Summary.—A complete analysis is given of the non-linear distortions due to the tracking error of the pick-up mechanism in the reproduction of lateral-cut disk recordings. The separate treatment of tracking distortion is permissible as long as the overall distortion of the reproduction is tolerable, the system being "almost linear," or the various distortion products superposable.

For the simplest case of a sinusoidal signal, it is possible to derive explicitly the whole Fourier spectrum of the reproduced signal, the mathematical proposition being the same as in the mechanical two-body problem. For general signals, an explicit operational expansion of the distorted signal is obtained.

As the kinematical effect of tracking error consists of an amplitude controlled advance and delay of the pick-up, the harmonic distortion may be characterized as made up of the side-bands of frequency modulation of the signal by itself. Compared with the ordinary type of non-linear distortion due to curved static characteristics, which may be correspondingly characterized as amplitude automodulation, the spectral character of tracking distortion stresses the higher frequency components. For second-order distortion which is prevalent, the emphasis is proportional to frequency.

The analysis shows, that both absolute and nuisance effects of tracking distortion are considerably greater than commonly assumed, published values usually being underestimates, due to omission of rigorous procedure. Tracking distortion is given approximately by the tracking error weighted with the inverse of the groove radius; the weighted error is referred to the mean groove radius of the record. The recording characteristic affects distortion products independently of their mechanisms.

Pick-up design as based on the analysis should reduce the weighted tracking error as much as possible. For optimal design, Tchebyshev approximation, commonly used in electric wave-filter design, is used. For straight arms, where only one design parameter, i. e., the underhang, is available, optimal approximation of zero distortion is of first order; for offset arms, where both offset angle and overhang are adjustable, it is of second order and thus much closer. The influence of deviations from optimal design due to errors of mounting is investigated as well as the combined effect of offset angle and stylus friction on the lifting force and its reduction by suitably modified design. The compromise design of multi-purpose arms is also treated. Simple design formulas are developed throughout, covering the various record sizes, speeds, and arm lengths. It is found that offset arms are much superior to straight arms. Track-

---

* Presented at the 1941 Spring Meeting at Rochester, N. Y.; received May 1, 1941.

** The Brush Development Co., Cleveland, Ohio.

ing distortion can be reduced to negligible magnitude with properly designed offset arms even under adverse conditions, such as short arm length and appreciable mounting tolerance.

The tracking mechanism commonly employed for the reproduction of disk recordings consists of an arm swinging about a vertical axis. For lateral recordings, the center of motion of the pick-up stylus is a horizontal axis pivoted in the head of the swing arm. By virtue of the kinematics of this system, the direction of the stylus tip motion does not, in general, coincide with the disk radius. The angular difference, which is equal to that between the direction of the pivotal axis and groove tangent, is known as "tracking error." Its magnitude and sign depend on the geometrical data of the system and on the radial position.

It is well known that the tracking error gives rise to distortions. Among the sources of non-linear distortion encountered in disk recording and reproduction, the tracking error is usually considered as entirely negligible. This, however, is not quite correct. The truth is that tracking distortion *can* be effectively eliminated in a simple way, *i. e.*, by proper geometrical design of the tone arm. Considerable deviations from optimum design, as are sometimes met in commercial pick-ups, lead, however, to quite serious distortions.

As tracking error is obnoxious only by virtue of the distortion caused, quantitative understanding of the effect is the necessary basis for tone arm design. Optimal design should minimize tracking distortion over the entire playing range of the record, which, as analysis shows, is by no means synonymous with minimizing the tracking error itself. Although this may sound commonplace, there is the fact that almost none of the numerous publications on the subject gives an analytic investigation of the effect. This omission frequently leads to erroneous results regarding optimum tone arm design, as in a recent paper by G. E. MacDonald;[1] or it leads to considerable underestimations of the magnitude of tracking distortion and of its nuisance effect which depends on its spectral character. This is the case in a frequently quoted paper by B. Olney[2] who gives a lucid qualitative description of the effect and considerable experimental material. E. G. Löfgren,[3] who first pointed out the error in reference *2* is, as far as the writer is aware, the only author who attacked the subject analytically and also discussed design questions on this basis.

The present paper gives a rigorous analysis of tracking distortion and develops the geometrical tone arm design on this basis.

Part I—Analytical Investigation of the Tracking Error Distortions

s = coördinate along the unmodulated groove
$y(s)$ = laterally recorded signal
$Y(s)$ = stylus elongation or reproduced signal
η = angular tracking error (radians or degrees)
e = distortion parameter
η' = weighted tracking error
} defined in the text
t = time
$v(t) = \frac{dy}{dt}$ = velocity of recorded signal
$V(t) = \frac{dY}{dt}$ = velocity of picked-up signal
Ω = angular disk speed in $\text{sec}^{-1} = \frac{\pi}{30} \times$ speed in rpm
r = radius of an arbitrary groove
r_1; r_2; $r_m = \sqrt{r_1 r_2}$ = inner; outer; mean groove radius of a disk record
ω = recorded angular frequency in sec^{-1}
y_0 = recorded amplitude
$v_0 = \omega y_0$ = recorded velocity amplitude
λ = recorded wavelength
φ = recorded phase
ψ = picked-up phase
} of a sinusoidal signal

(*a*) *General Considerations.*—Fig. 1 gives a picture of the stylus motion. The curve $y(s)$ represents the center line of the laterally displaced groove or the recorded signal. Due to the angular error η, the instantaneous position of the stylus tip P becomes S' instead of S, *i. e.*, its abscissa is displaced by Δs. The relation between the recorded elongation $y(s)$, the picked-up elongation $Y(s)$, and the instantaneous shift Δs is evidently

$$Y(s) = \sec \eta \cdot y(s + \Delta s); \quad \Delta s = \tan \eta \cdot y(s + \Delta s) \qquad (1)$$

Kinematically, the effect thus constitutes an alternating advance and delay of the reproduced signal with respect to the recorded one, or a "frequency modulation" of the signal by itself. The associated harmonic distortion can be interpreted as the "side-bands" of this auto-modulation. This interpretation may prove helpful for the understanding of the results of the analysis. It leads to the anticipatory result that, due to the increased depth of frequency auto-modulation, harmonic distortion of a given signal should increase with decreasing groove velocity. For a given distortion limit, larger

tracking error should thus be permissible at the outer grooves of a record than at its inside. This is confirmed by analysis.

Fig. 1 represents idealized conditions, as the finite dimensions of groove and stylus tip are neglected. As kinematic implication, the effects connected with the groove geometry, which give rise to tracing distortion,[4] are thus ignored. As mechanical implication, the elastic deformations caused by the bearing weight and the lateral stiffness and inertia forces, are neglected. They lead to both linear and non-linear distortions, but only the former have been investigated so far.[5] They are referred to as "playback loss."[5] While in the strict sense, tracking distortion and harmonic distortion from other sources inherent in the playback process, are interdependent, they can be

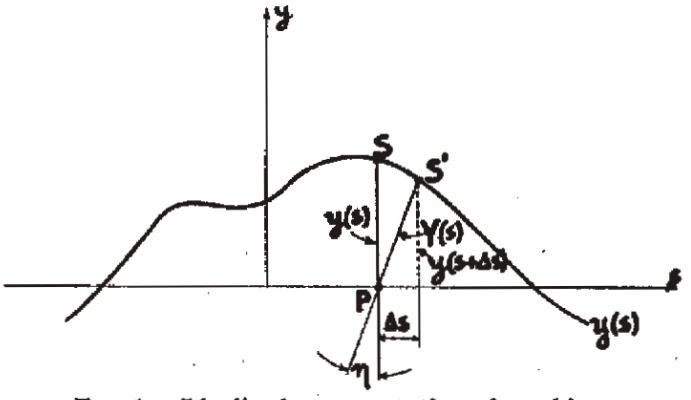

FIG. 1. Idealized representation of tracking.

treated as superposable under practical conditions, *i. e.*, as long as the square of relative overall harmonic distortion is small compared with 1. This corresponds to "almost-linearity" as put forward by Feldtkeller and others.[6] Thus the idealized picture represented by Fig. 1 and equation *1* is usually adequate for the treatment of tracking distortion, if $y(s)$ signifies the signal as modified by the linear effects.* As the playback loss is usually positive, the neglected effects would tend to reduce tracking distortion.

(*b*) *Rigorous Solution for a Sinusoidal Signal; Bessel's Solution of the Kepler Problem.*—The relation *1* is an implicit equation involving

* It is further assumed that no tracking error is introduced by the cutter. The distortions due to angular error of the cutting tool which may be present in home recorders, are of a more complicated character and will be treated in a separate paper.

the unknown shift Δs. In order to obtain from it the tracking distortion explicitly, the picked-up signal $Y(s)$ has to be expressed in terms of the recorded one, $y(s)$. The desired result will be obtained in the form of an operational expansion, similarly as in other cases of calculation of modulation products.[7] Before, however, taking up the general case of complex signals, we shall deal first with the simplest case, *i. e.*, with a sinusoidal signal

$$y(s) = y_0 \sin \frac{2\pi}{\lambda} s \equiv y_0 \sin \varphi, \tag{2}$$

for which the solution of equation *1* can be obtained in closed form.

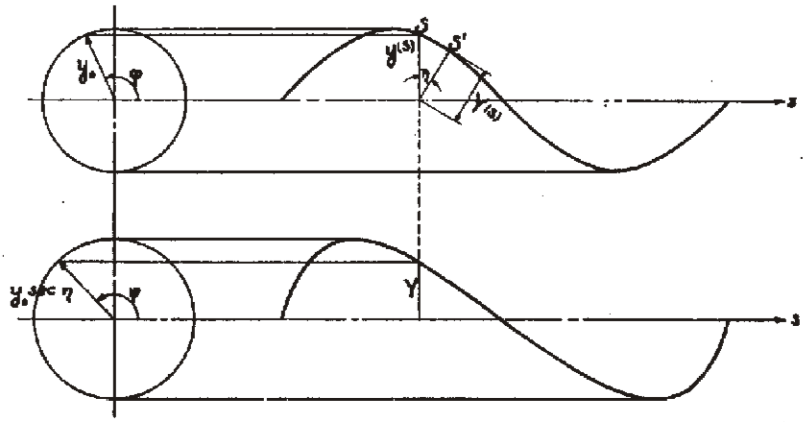

FIG. 2. Geometrical construction for sinusoidal signals.

The picked-up signal can be described correspondingly by means of a phase angle ψ:

$$Y(s) = y_0 \sec \eta \sin \psi(s) \tag{3}$$

The simple graphical construction of *3* from *2* according to equation *1* is carried out in Fig. 2 for an exaggerated case ($\eta = 30°$), in order to make the distortion plain. The corresponding implicit relation is evidently:

$$\psi - \epsilon \sin \psi = \varphi; \quad \epsilon \equiv 2\pi \frac{y_0}{\lambda} \tan \eta = \text{distortion parameter.} \tag{4}$$

Introducing time as the independent variable, by means of the relation

$$s = r\Omega t; \quad \frac{\lambda}{2\pi} = \frac{r\Omega}{\omega}, \tag{5}$$

it follows

$$y(t) = y_0 \sin \omega t \equiv y_0 \sin \varphi \tag{2a}$$

and

$$\text{distortion parameter } \epsilon = \frac{y_0 \omega}{r\Omega} \tan \eta \equiv \frac{v_0 \tan \eta}{r\Omega}, \tag{4a}$$

where v_0 denotes the recorded velocity amplitude while $r\Omega$ is the longitudinal groove velocity.

As a matter of historical interest, it is worth pointing out that the solution of eq. 4 or Fourier expansion of ψ in terms of φ, *i. e.*, the tracking distortion of a sinusoidal signal proves to be the same mathematical proposition as the classical two-body problem of celestial mechanics (Kepler problem), which involves the description of the (undisturbed) motion of a planet about the sun in terms of the phase of its period of revolution. This is briefly illustrated in Fig. 3 which shows the Kepler ellipse with the half-axes a and b and the foci S and S', representing the orbit of a planet P about the sun S;* the generating circle of radius a is also shown. The numerical eccentricity of the ellipse is $\epsilon = \sqrt{1 - (b/a)^2}$. The instantaneous position of the planet is usually characterized by the focal phase ϑ or by the central angle ψ (both measured from the apex A), the so-called "true anomaly" and "eccentric anomaly," respectively. Quantitative description of the planetary motion requires an expression of these angles in terms of time t or of the phase angle ("mean anomaly") $\varphi = 2\pi t/T$ (T = period of revolution). From the well known geometrical relations between focal radii and anomalies:

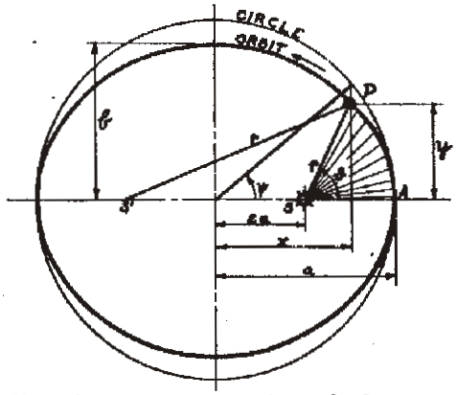

FIG. 3. Representation of planetary motion.

$$r = a(1 - \epsilon \cos \psi); \tan \frac{\vartheta}{2} = \sqrt{\frac{1+\epsilon}{1-\epsilon}} \tan \frac{\psi}{2}; \sin \psi = \frac{\sqrt{1-\epsilon^2} \sin \vartheta}{1 + \epsilon \sin \vartheta}, \text{ etc.},$$

and from the dynamical theorem of the invariance of the momentum

* Actually, S represents the center of gravity of sun and planet; as, however, the mass of the sun is usually very large compared to that of a planet, the difference will be negligible.

vector (Kepler's second law), which requires the orbital area (shaded in Fig. 3) to be equal to the mean anomaly:

$$\pi \int_0^{\vartheta} r^2(\vartheta) d\vartheta = 2\pi \frac{t}{T} \equiv \varphi,$$

there follows, by elimination of ϑ, at once the relation

$$\psi - \epsilon \sin \psi = \varphi. \qquad (4')$$

This is identical with *4* and *4a;* eccentricity, mean, and eccentric anomaly correspond to distortion parameter, phase of the recorded, and phase of the picked-up signal, respectively. Equation *4'* was first given by Lagrange[8] in a famous memoir in 1770; he obtained power expansions of the first three Fourier coefficients of $\sin \psi$. The complete solution of the problem (including the Fourier analysis of ϑ and r) was obtained by Bessel[9] in 1824 in a classical investigation where he introduced his well known integral representation, and which is considered as the beginning of the modern theory of Cylinder Functions. (For historical notes see Chapter I, Part 1.4 of Watson's *Treatise.*[10])

The solution of *4* follows at once upon application of the Bessel-Sommerfeld integral (see[10] Chapter VI, or,[11] or [12]); it may be found, together with related results, in Chapter XVII (Kepteyn Series), No. 17.2, pp. 551–558 of Watson's *Treatise;*

$$Y = \frac{v_0}{\omega} \sec \eta \cdot \sum_{n=1}^{\infty} \frac{J_n(n\epsilon)}{{}^1/_2 n\epsilon} \sin n\omega t; \quad \frac{dY}{dt} \equiv V(t) = v_0 \sec \eta \cdot \sum_{n=1}^{\infty} \frac{J_n(n\epsilon)}{{}^1/_2 \epsilon} \cos n\omega t \qquad (6)$$

(J_n denotes the Bessel function of nth order.)

Apart from the factor sec η, the relative amplitude a_1 of the fundamental frequency is thus $J_1(\epsilon)/{}^1/_2\epsilon$, those a_n and b_n of the nth harmonic, $J_n(n\epsilon)/{}^1/_2 n\epsilon$ and $J_n(n\epsilon)/{}^1/_2\epsilon$, for the picked-up elongation and velocity, respectively. The relative harmonic distortion is defined by the rms values

$$\sqrt{\frac{\sum_{n=2}^{\infty} a_n^2}{\sum_{n=1}^{\infty} a_n^2}} \equiv \sqrt{1 - \frac{a_1^2}{\sum_{n=1}^{\infty} a_n^2}} \text{ and } \sqrt{1 - \frac{b_1^2}{\sum_{n=1}^{\infty} b_n^2}}, \text{ respectively.}$$

By virtue of the well known relation

$$\sum_1^\infty a_n^2 = \frac{1}{\pi}\int_{(2\pi)} Y^2(\psi)d\varphi, \sum_1^\infty b_n^2 = \frac{1}{\pi}\int_{(2\pi)} Y^2(\psi)d\varphi,$$

we obtain

$$\sum_1^\infty a_n^2 = \left(\frac{v_0}{\omega}\sec\eta\right)^2 \cdot \frac{1}{\pi}\int_{(2\pi)} \sin^2\psi d\varphi = -\left(\frac{v_0}{\omega}\sec\eta\right)^2 \cdot \frac{1}{\pi}\int_{(2\pi)} \sin(2\psi)\varphi d\psi = \left(\frac{v_0}{\omega}\sec\eta\right)^2$$

by virtue of *4*. Similarly,

$$\sum_1^\infty b_n^2 = (v_0\sec\eta)^2 \cdot \frac{1}{\pi}\int_{(2\pi)}\left(\cos\psi\frac{d\psi}{d\varphi}\right)^2 d\varphi =$$

$$(v_0\sec\eta)^2 \frac{1}{\pi}\int_{(2\pi)} \frac{\cos^2\psi}{1-\epsilon\cos\psi}\,d\psi = \frac{(v_0\sec\eta)^2}{\sqrt{1-\epsilon^2}\cdot{}^1/_2(1+\sqrt{1-\epsilon^2})}$$

Therefore relative harmonic distortion

$$\left.\begin{aligned} \text{of } Y\text{:}\ & \sqrt{1-\left(\frac{J_1(\epsilon)}{{}^1/_2\epsilon}\right)^2} = \frac{\epsilon}{2}\left(1-\frac{5}{24}\left(\frac{\epsilon}{2}\right)^2+\frac{31}{1152}\left(\frac{\epsilon}{2}\right)^4\cdots\right) \\ \text{of } V\text{:}\ & \sqrt{1-\sqrt{1-\epsilon^2}\cdot\frac{1+\sqrt{1-\epsilon^2}}{2}\cdot\left(\frac{J_1(\epsilon)}{{}^1/_2\epsilon}\right)^2} = \epsilon\left(1-\frac{29}{96}\left(\frac{\epsilon}{2}\right)^2+\right. \\ & \left.\qquad\qquad \frac{4567}{18432}\left(\frac{\epsilon}{2}\right)^4\cdots\right) \end{aligned}\right\} \quad (7)$$

(*c*) *Discussion—The Prevalent Type of Distortion.*—Equation *7* shows that if the relative rms distortion is restricted to moderate values, the 1st term alone: $\epsilon/2$ or ϵ, on the basis of elongation or velocity, respectively, gives a satisfactory approximation. The next higher term is negligible for overall distortions even as high as 50 per cent. The first term represents the relative amplitude of the second order harmonic a_2 or b_2, respectively; this is seen from *6* upon substituting for the Bessel coefficients the initial terms of their power expansions. The relative amplitudes of the higher-order harmonics are of corresponding order in ϵ; they are

$$\frac{({}^1/_2 n\epsilon)^{n-1}}{n!} \text{ and } \frac{({}^1/_2 n\epsilon)^{n-1}}{(n-1)!}, \text{ respectively.}$$

Under normal conditions, the distortion is therefore essentially of second order. For complex signals, the 2nd-order cross-modulation products will thus be the prevalent distortion components.

(*d*) *Distortion Spectrum of Complex Signals.*—For general signals, a solution of *1* in closed form does not exist. Expansional solution is thus called for and can be expected to converge satisfactorily, in view of the rapid convergence of the expansions in case of sinusoidal signals. The implicit form of equation *1* would require an approach by iteration; it is possible, however, to obtain the final result at once by means of a well known expansion theorem due to Lagrange[13, 14*] which is a special case of Teixeira's Theorem.[14] The simple intermediate calculation is omitted. The result is analogous to that for the sinusoidal signal, eqs. *6* and *7*, the relevant quantity, *i. e.*, the distortion parameter $\epsilon = (\omega y_0/r\Omega)$ being replaced by the distortion operator $\tan \eta/r\Omega \frac{d}{dt}$ applied to $y(t)$:

$$\left.\begin{aligned} \cos\eta \cdot V(t) = y(t+\Delta t) &= \sum_{n=1}^{\infty} \frac{1}{n!}\left(\frac{\tan\eta}{r\Omega}\frac{d}{dt}\right)^{n-1}\{(y(t))^n\} \\ \cos\eta \cdot V(t) &= \frac{r\Omega}{\tan\eta}\cdot\sum_{n=1}^{\infty}\frac{1}{n!}\left(\frac{\tan\eta}{r\Omega}\frac{d}{dt}\right)^{n}\{(y(t))^n\} \end{aligned}\right\} \qquad (8)$$

or symbolically:

$$\cos\eta \cdot V(t) = \frac{r\Omega}{\tan\eta}\left[e^{\left\{\frac{\tan\eta}{r\Omega}\frac{d}{dt}\right\}(y(t))} - 1\right]. \qquad (8a)$$

(For sinusoidal signals, *8* is re-obtained from *6* by means of the power expansion of the Bessel Functions—as it must be.)

Similar considerations as in the case of a sinusoidal signal show that, for moderate overall distortion, the first term, which represents second-order distortion is in general predominant:

$$\left.\begin{aligned} \cos\eta \cdot V(t) - y(t) &= \frac{\tan\eta}{r\Omega}\frac{d}{dt}\left(\frac{y^2}{2}\right) + \cdots \\ \cos\eta \cdot V(t) - v(t) &= \frac{\tan\eta}{r\Omega}\frac{d^2}{dt^2}\left(\frac{y^2}{2}\right) + \cdots \end{aligned}\right\} \qquad (8b)$$

For the ordinary type of non-linear distortion as met in tubes, *etc.*, the distortion terms corresponding to *8b* would be const. $y^2/2$ and const. $(d/dt)(y^2/2)$, respectively. It will be appreciated that it is

* The convergence conditions are automatically fulfilled by virtue of the limitation of the frequency spectrum inherent in the recording process: $y(s)$ is, therefore, continuous and of bounded oscillation.

appropriate to interpret the two cases as amplitude and frequency auto-modulation. In order to illustrate the difference between the two associated distortion spectra, let us consider the simple two-component signal*

$$y(t) = y_1 \sin \omega_1 t + y_2 \sin \omega_2 t \qquad (9)$$

For the case of ordinary second-order distortion, we obtain, in addition to y itself, the following distortion components:

Frequency	0	$2\omega_1$	$2\omega_2$	$\lvert\omega_1 - \omega_2\rvert$	$\omega_1 + \omega_2$
Amplitude	$\frac{c}{2}(y_1^2 + y_2^2)$	$\frac{c}{2}y_1^2$	$\frac{c}{2}y_2^2$	cy_1y_2	cy_1y_2

where c denotes the second expansion coefficient of the normalized non-linear characteristic. For the second-order tracking error distortion of the same signal, we obtain from *8b*

Frequency	0	$2\omega_1$	$2\omega_2$	$\lvert\omega_1-\omega_2\rvert$	$\omega_1 + \omega_2$
Amplitude	0	$\frac{\tan\eta}{r\Omega}\omega_1\frac{y_1^2}{2}$	$\frac{\tan\eta}{r\Omega}\omega_2\frac{y_1^2}{2}$	$\frac{\tan\eta}{r\Omega}\lvert\omega_1-\omega_2\rvert\frac{y_1y_2}{2}$	$\frac{\tan\eta}{r\Omega}(\omega_1+\omega_2)\frac{y_1y_2}{2}$

It is seen that the amplitudes of the distortion components are weighted with their respective frequencies, relative to the former case; this corresponds to the application of d/dt. Comparison on the velocity basis, which is more appropriate to the major part of the conventional recording characteristic, gives the corresponding result

Frequency	$2\omega_1$	$2\omega_2$	$\lvert\omega_1 - \omega_2\rvert$	$\omega_1 + \omega_2$
Amplitude, ord. dist.	$c\frac{v_1^2}{\omega_1}$	$c\frac{v_2^2}{\omega_2}$	$c\frac{\lvert\omega_1 - \omega_2\rvert}{\omega_1\omega_2}v_1v_2$	$c\frac{\omega_1 + \omega_2}{\omega_1\omega_2}v_1v_2$
Amplitude, track. error	$\frac{\tan\eta}{r\Omega}v_1^2$	$\frac{\tan\eta}{r\Omega}v_2^2$	$\frac{\tan\eta}{r\Omega}\frac{(\omega_1 - \omega_2)^2}{2\omega_1\omega_2}v_1v_2$	$\frac{\tan\eta}{r\Omega}\frac{(\omega_1 + \omega_2)^2}{2\omega_1\omega_2}v_1v_2$

* Löfgren[3] carries out, and points out the salient results of, the multi-component signal analysis, but he does not give the general expansion *8*, *8a*. Application of the Laplace integral (spectrum analysis) to the general expansion *8* would yield the spectra of the distortion components of nth order of signals with continuous and/or line spectra. The character of such distortion spectra was studied and discussed by Lewis and Hunt[4] for the tracing distortions. It could easily be carried out in the same way for tracking distortion, but this does not lead to any fundamentally new conclusions pertinent to tone-arm design, beyond those based on the simple case *9*. It should be mentioned, however, that the spectrum of lateral tracing distortion, which is of odd order only, is weighted with a power of frequency still higher—by one—than that of tracking distortion.

(*e*) *Nuisance Effect of Distortion; Influence of Recording Characteristic; Permissible Size of Tracking Error; Weighted Tracking Error.*— The definition of the distortion parameter ϵ (eq. 4*a*) can easily be extended to the two-component signal 9. In particular, for $y_1 = y_2$:

$$y = y_0(\sin \omega_1 t + \sin \omega_2 t), \tag{9a}$$

we obtain

$$\epsilon_0 = \frac{\tan \eta \cdot y_0 \omega_0}{r\Omega}; \quad \omega_0 \equiv \sqrt{\omega_1 \omega_2} \tag{4b}$$

Let us compare the second-order ordinary-type and tracking distortions of 9*a* on a common basis, *i. e.*, for equal rms values, whereby the d-c component is not counted as it is without significance for electroacoustic purposes. The ratio of the distortion parameters c and ϵ_0 then becomes

$$\frac{c}{\epsilon_0} = \sqrt{0.3(a + a^{-1})}; \quad a \equiv \frac{\omega_2}{\omega_1}$$

This gives, apart from a common factor, the following values for the amplitudes of the distortion components:

Frequency	$2\omega_1$	$2\omega_2$	$\lvert\omega_1 - \omega_2\rvert$	$(\omega_1 + \omega_2)$
Ord. type	$\sqrt{0.3(a + a^{-1})}$	$\sqrt{0.3(a + a^{-1})}$	$2\sqrt{0.3(a + a^{-1})}$	$2\sqrt{0.3(a + a^{-1})}$
Tr. err.	$\frac{1}{\sqrt{a}}$	$\sqrt{a}$	$\sqrt{a} - \frac{1}{\sqrt{a}}$	$\sqrt{a} + \frac{1}{\sqrt{a}}$

If (ω_1, ω_2) represents a consonant musical interval, the second-order modulation products are also consonant with it, with the possible exception of the summation tone. For instance, for a Fourth with $a = {}^4/_3$ (in the natural scale; $2^{5/12} = 1.3347$ according to equal temperament), the difference tone is 2 octaves below ω_2, *i. e.*, consonant, while the frequency of the summation tone is ${}^7/_6$ times that of the octave of ω_1; this does not represent an interval of the musical scale and is therefore dissonant. For unity rms value, the relative amplitudes are in this case:

Frequency	$2\omega_1$	$2\omega_2$	$\lvert\omega_1 - \omega_2\rvert$	$(\omega_1 + \omega_2)$
Ord. type distortion	0.316	0.316	0.632	0.632
Track. err. distortion	0.346	0.462	0.115	0.808

This is represented in Fig. 4.

The preceding considerations show that the spectral character of tracking distortion is roughly taken into account on the velocity basis. This means that the distortion parameter ϵ as originally defined for sinusoidal signals gives a fair estimate of the relative tracking distortion produced by complex signals, if ω signifies a dominant frequency range and y a suitable average amplitude. (If the distortion were of the ordinary type, $\epsilon/2$ would have to be used instead.)

The spectral character of all kinds of harmonic distortion produced in the playback process is uniformly modified by the playback frequency characteristic which is the inverse of the recording character-

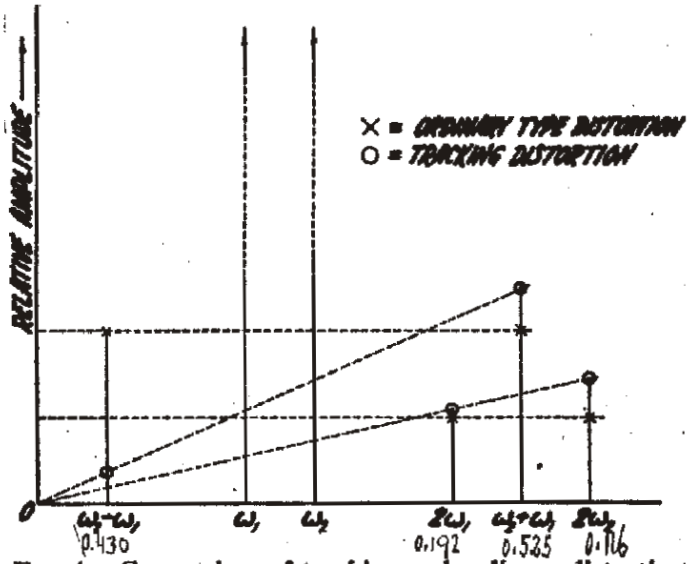

FIG. 4. Comparison of tracking and ordinary distortion spectra of a two-component signal.

istic. In case of the conventional constant-velocity characteristic, for instance, distortion components are emphasized, in playback, proportionally to their respective frequencies.* It can be generally shown that, for any particular distortion term, the effects of the playback characteristic and of the distortion mechanism itself simply superpose; the relative amplitude of any resulting distortion component is thus the product of two mutually independent factors. For instance, the relative amplitude of the second-order distortion component of frequency ω_p, which is produced by the two signal com-

* The emphasis of the constant-velocity characteristic on the higher distortion components is stressed in Guttwein's paper.[5]

ponents of frequencies ω_a and ω_b, is proportional to $F(\omega_a;\ \omega_b;\ \omega_p)\cdot\frac{f(\omega_a)f(\omega_b)}{f(\omega_p)}$ where $f(\omega)$ denotes the recording characteristic and $F(\omega_a;\ \omega_b;\ \omega_p)$ accounts for the distortion mechanism; in case of tracking distortion, F is given by the second table following 9.

The physiological effect of harmonic distortion of a given rms value is usually increased by high-frequency emphasis.[15] It follows that tracking distortion—in particular as produced by signal components of large amplitude in the upper middle audio range—will have a relatively high nuisance effect, not adequately accounted for on the elongation basis.[2]

The preceding analysis and discussion of tracking distortion furnishes the basis for rational pick-up design. In order to have a fixed aim, it is useful to set a limit of permissible tracking distortion, in terms of the distortion parameter ϵ. This limit should be kept low, for three reasons: (*1*) The nuisance value of tracking distortion is likely to be increased on account of high-frequency emphasis; (*2*) an amount of harmonic distortion too small to be troublesome by itself, may become so when superposed upon distortion which is already appreciable. This is the case here, due to the presence of harmonic distortions obtained in cutting, pressing, and playback, more often than not in objectionable amounts; (*3*) while, in the present state of the art, the overall effect of these distortions, whose mechanisms are still partly unexplained, can not be reduced below nuisance level under commercial conditions, it is possible to eliminate tracking distortion substantially by proper tone arm design.

For these reasons, an upper limit of harmonic distortion—as represented by $|\epsilon|$, the absolute value of the distortion parameter—of only 2 per cent is postulated for a signal level of 8 cm/sec velocity amplitude, over the whole playing range of any record size and speed for which an arm is designed. This corresponds to 1 mil elongation at 500 cps and represents approximately maximum conditions in transcription and about half the permissible amplitude in commercial recordings.

The two conventional speeds and associated playing ranges are $33^1/_3$ rpm, $r_{1\ \min} \sim 3^1/_2$ inches, $r_{2\ \max} \sim 8$ inches for transcription and 78 rpm, $r_{1\ \min} \sim 2$ inches, $r_{2\ \max} \sim 6$ inches for commercial disks. The associated minimum and maximum groove velocities are 31 and $41^1/_2$ cm/sec, and 71 and 124 cm/sec, respectively. With the limit set for $|\epsilon|$, the maximum value of $|\tan \eta|$ occurring under any conditions

is then 0.3, according to *4a*. It will be seen later that it is usually considerably smaller. It is thus permissible to neglect $\eta^2/2$ against 1, *i. e.*, to put

$$\tan\eta \doteq \eta \doteq \sin\eta, \cos\eta \doteq 1 : |\epsilon| = \frac{v|\eta|}{r\Omega}. \qquad (10)$$

As tracking distortion is inversely proportional to the groove radius, it is preferable to use for design purposes the

$$\text{weighted tracking error } \eta' \equiv \frac{r_m}{r}\cdot\eta \qquad (11)$$

which is referred to the mean groove radius r_m, rather than η itself. Distortion is then proportional to η', independently on the radius r. The factor of proportionality becomes 17 for transcription recordings with $v_{max} \sim 8$ cm/sec, 22 for commercial disks with $v_{max} \sim 16$ cm/sec.

$$\text{Distortion } |\epsilon|_{max}(\text{in per cent}) \sim (17 \text{ to } 22)\cdot|\eta'| \text{ (in radians)}. \qquad (12)$$

For $|\epsilon|_{max} = 2$ per cent at $v = 8$ cm/sec, it is thus $|\eta'|_{max} \sim 0.12$ and 0.18 for transcription and commercial conditions, respectively. For the tracking error itself the following upper limits are obtained: $4\frac{1}{2}$ to 10° for transcription, 6 to $17\frac{1}{2}$° for commercial disks, for $r = r_{1\,min}$ to $r = r_{2\,max}$.

PART II—PICK-UP DESIGN FOR MINIMUM TRACKING ERROR DISTORTIONS

Additional notations

L = length of tone arm (swing axis to stylus tip)
$L + d$ = distance between turntable axis and swing arm axis } (see Fig. 5)
(d is called "underhang" if >0, "overhang" if <0)

$\delta \equiv \frac{d}{L}$ = numerical under- or overhang

$x \equiv \frac{r}{L}$ = numerical groove radius; $x_{1;\,2;\,m} \equiv \frac{r_{1;\,2;\,m}}{L}$

$a \equiv \frac{r_2}{r_1}$; $p \equiv \frac{1}{2}\left(\sqrt{a} + \frac{1}{\sqrt{a}}\right) = \frac{x_1 + x_2}{2x_m}$

$\eta'_{1;2}$ = weighted tracking error for $r_{1;\,2}$; $\eta'_0 \equiv \eta'(x_0)$ = extremum of the weighted tracking error

γ = angle between groove tangent and line from stylus tip to swing axis

α = angle between direction of pivotal axis of stylus and line from stylus tip to swing axis—"offset angle"

δ_{opt}; d_{opt}; α_0; α_{opt}; α_{crit}; α': explained in text

$T_n(x)$ = Tchebychev polynomial of nth order

P = bearing weight of stylus
F = longitudinal friction force between stylus and groove
F_h = horizontal centripetal component } explained in text
F_v = vertical component
ρ = coefficient of friction between stylus and record groove
} in grams

(*a*) *Geometrical Relations; Tchebychev Method of Approximation.*— The geometrical conditions are represented in Fig. 5 for both straight arms (left side) and arms with offset head (right side). In both cases, C represents the axis of the turntable, A that of the swing-arm, P the stylus point, and D the intersection of arm radius with the line CA.

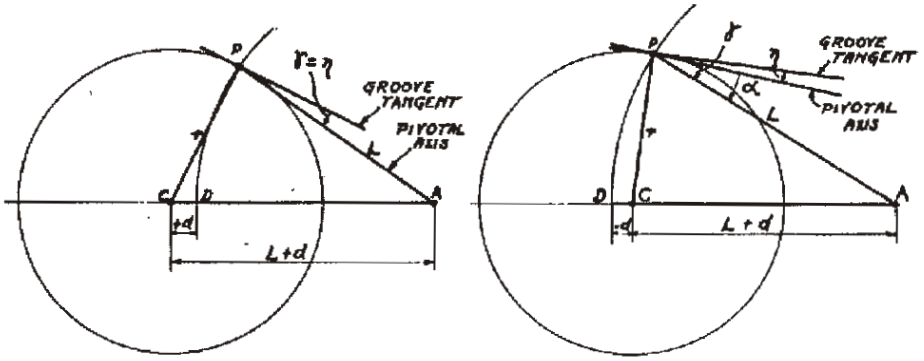

FIG. 5. Geometry of straight and offset tone arms.

It is

$$\left.\begin{aligned} &\sin\eta = \sin\gamma = \frac{r^2 - 2d - d^2}{2r} \equiv \frac{x^2 - 2\delta - \delta^2}{2x}\ (\delta > 0), \text{ for the straight arm} \\ &\eta = \gamma - \alpha, \sin\gamma = \frac{x^2 - 2\delta - \delta^2}{2x}\ (\delta < 0), \text{ for the offset arm} \end{aligned}\right\} \quad (13)$$

With the approximation *10*, this gives for the weighted tracking error η', according to *11*:

$$\left.\begin{aligned} &\eta' = \frac{x_m}{2}\left(1 - \frac{2\delta + \delta^2}{x^2}\right), \text{ for straight arms} \\ &\eta' = \frac{x_m}{2\cos\alpha}\left(1 - \frac{2\delta + \delta^2}{x^2} - \frac{2\sin\alpha}{x}\right), \text{ for offset arms} \end{aligned}\right\} \quad (14)$$

An arm that is designed optimally for a single speed and record size, will be called single-purpose arm; otherwise we speak of multi-purpose arms. Single-purpose arms will be treated first.

The design should minimize tracking distortion over the whole playing range by suitable choice of the design parameters. In case of

straight arms, only one parameter is available, *i. e.*, the underhang, whose optimal value turns out to be positive under any conditions (Fig. 5, *left*). Offset arm design has two parameters available, *i. e.*, offset angle and underhang; it turns out that for optimal design, the latter is always negative, and thus constitutes an overhang (Fig. 5, *right*). The result, namely the tracking distortion for optimal design, will appear in terms of the arm length. This will yield the minimal length compatible with a prescribed distortion limit.

The design reduces to elementary procedure as soon as a definition of minimum distortion over the playing range is agreed upon; in other words, we have to decide, which function $\eta'(x)$ containing the parameters α and δ (or δ alone in case of the straight arm) should represent the "best" approximation of the ideal $\eta' \equiv 0$ in the playing interval $x_1 \leqslant x \leqslant x_2$. In general, the success of the approximation, in a prescribed interval, of a given function by another that contains adjustable parameters, can be judged by different criteria. For instance, minimal rms value of the difference may be postulated (this would imply the well known method of least squares). More generally, any monotonic increasing function of the difference, integrated over the fundamental interval, could be chosen as criterion. In particular, this "weight function" by which the seriousness of local deviation is gauged, could be chosen as zero below a certain limit which should be made as small as possible, and very large above this limit; in this case, that approximation is considered best, for which the maximum of the absolute difference between the two functions or their "tolerance" becomes minimum. This mode of approximation was proposed and investigated by Tchebychev[17] and has recently found increasing application in engineering, *e. g.*, in the design of electric wave-filters.[18,19] Tchebychev's approximation is appropriate whenever deviation becomes rapidly objectionable beyond a certain limit. This applies, more or less, to the nuisance value of harmonic distortions. It seems therefore that the tone-arm design should be carried out in the Tchebychev manner, provided that the associated calculations are not unduly complicated. They will actually prove to be of satisfactory simplicity. As a matter of fact, the relation *14* is so simple that almost any mode of approximation could be used on that account. While the design is not greatly altered when applying different types of approximation, it seems that the Tchebychev manner is somewhat preferable to the minimal mean square suggested by Löfgren.[3]

Tchebychev has proved that under rather general conditions the smallest tolerance between the given and the approximation function is obtained if the available parameters are so adjusted that the difference alternates as many times as possible in the given interval between the positive and negative tolerance. This is precisely the result one would expect. The point is illustrated in Fig. 6, which shows the graphs of the first four Tchebychev polynomials $T_n(x)$; $n = 1...4$, defined as those polynomials of nth degree with the coefficient 1 of x^n, which approximate the function $x = 0$ with the smallest tolerance in the interval $-1 \leqslant x \leqslant +1$. They are[17,20]

$$T_n(x) = 2^{-(n-1)} \cos (n \cdot \arccos x);$$

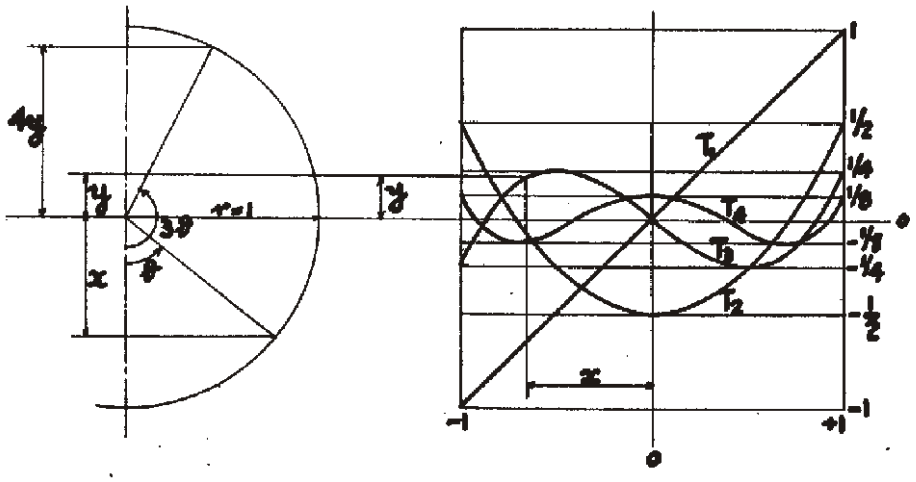

FIG. 6. Plots of the first four Tchebyshev polynominals and their geometrical construction.

i. e., $T_n(x)$ oscillates between the tolerances $\pm 1/2^{n-1}$, reaches them at the $n + 1$ locations $x_k = \cos k\pi/n$; $k = 0, 1, \ldots, n$, and goes through zero at the n points $x_m = \cos (m - 1/2)\pi/n$, $m = 1, 2, \ldots, n$.

In the general case where the approximation functions are not polynomials and this symmetry is no longer present, nth-order approximation is still characterized by the fact that the tolerance is reached $(n + 1)$ times, including the ends of the interval. In general, the order of the approximation is equal to the number of available parameters. Consequently, the best approximation to be expected for straight arms is, in general, of 1st order, with η' running from $-\eta'_{max}$ at $r = r_1$ through 0 to $+\eta'_{max}$ at $r = r_2$, the distortion being equal and maximum at the ends of the record; in this way, the smallest maximum distortion is realized. For the offset arm, second-order

approximation should be obtainable with the tracking error passing twice through zero and the distortion reaching the maximum value three times, *i. e.*, for r_1 and r_2 and an intermediate radius r_0. Considerably smaller values of distortion can be expected for the offset arm.

(*b*) *Single-Purpose Straight Arm Design.*—Tchebychev approximation of the underhang in eq. *14* for $\alpha = 0$ gives the following results:

Optimal underhang

$$\delta_{opt} = \sqrt{1 + \frac{x_m^2}{2p^2 - 1}} - 1 \doteq \frac{x_m^2}{2(2p^2 - 1)}; \quad d_{opt} \doteq \frac{r_1^2 r_2^2}{L(r_1^2 + r_2^2)} \tag{15a}$$

Maximal weighted tracking error

$$|\eta'_1| = |\eta'_2| \equiv |\eta'|_{max} = \frac{x_m}{2} \cdot \frac{a^2 - 1}{a^2 + 1} \equiv \frac{\sqrt{r_1 r_2}}{2L} \cdot \frac{r_2^2 - r_1^2}{r_2^2 + r_1^2} \tag{15b}$$

Maximal harmonic distortion, according to *12*

$$|\epsilon|_{max}\ (\%) \sim (8 \text{ to } 11) \cdot \frac{\sqrt{r_1 r_2}}{L} \cdot \frac{r_2^2 - r_1^2}{r_2^2 + r_1^2} \tag{15c}$$

Weighted tracking error as function of groove radius

$$\frac{\eta'}{|\eta'|_{max}} = \frac{1/2(a + a^{-1}) - \left(\frac{x_m}{x}\right)^2}{1/2(a - a^{-1})} \equiv \frac{r_2^2 + r_1^2 - 2\frac{r_1^2 r_2^2}{r^2}}{r_2^2 - r_1^2} \tag{15d}$$

Distortion vanishes at $r = \dfrac{r_1 r_2}{\sqrt{1/2(r_1^2 + r_2^2)}}$ (15e)

In Fig. 7, equation *15d* is plotted as $\eta'/|\eta'|_{max}$ *vs.* $x/x_m = r/\sqrt{r_1 r_2}$ for the three values $a = 2$, 3, and 4. When inserting the numerical values of the playing ranges of transcription and commercial disks, as given at the end of Part I, one obtains

$$|\epsilon|_{max}\ (\%) \sim \frac{30 \text{ to } 31}{L_{(\text{inches})}}. \tag{15f}$$

This shows that for correct mounting, distortion can just be kept within the limits set previously for commercial recordings with the conventional arm length of 8 inches, while for high-fidelity achievement in transcription, L should be not less than about 15 inches for a straight arm. For these conditions, the actual tracking error becomes about 4.5° at the extreme inner, about 10.3° at the outer groove for transcription, and about 5.9° and 17.8°, respectively, for commercial recordings.

Incorrect mounting may increase tracking distortions considerably. The quantitative influence will be discussed later on for both straight

and offset arms. It will be found that, for straight arm mounting, conditions are much more critical at the inner end than at the outer end of the playing range, and that therefore a mounting error which reduces the underhang slightly below the optimal value *15a* is much less harmful than an increase by the same amount. For instance, for an 8-inch arm and 12-inch disks, equation *15a* gives $d_{opt} = 0.438$ inch $\doteq {}^{7}/_{16}$ inch. It is found that an increase by only ${}^{1}/_{16}$ inch would increase the maximal distortion by 33 per cent. A decrease of d by the same amount, however, would increase $|\epsilon|_{max}$ by only 3.7 per cent. It is thus safe to keep somewhat below rather than above the optimal overhang.

(*c*) *Single-Purpose Offset Arm Design.*—The second-order Tchebychev approximation gives the following optimal values:

Optimal offset

$$\sin \alpha_{opt} = \frac{2px_m}{p^2+1} \equiv \frac{r_2+r_1}{L\left[\frac{\left(\frac{r_2+r_1}{2}\right)^2}{r_2r_1}+1\right]} \qquad (16a)$$

Optimal overhang

$$-\delta_{opt} = 1 - \sqrt{1-\frac{2x_m^2}{p^2+1}} \doteq \frac{x_m^2}{p^2+1}; \quad -d_{opt} \doteq \frac{r_2r_1}{L\left[\frac{\left(\frac{r_2+r_1}{2}\right)^2}{r_2r_1}+1\right]} \qquad (16b)$$

Maximal weighted tracking error; maximal harmonic distortion

$$\left.\begin{aligned} |\eta'|_{max} &= \frac{p^2-1}{p^2+1}\cdot\frac{x_m}{2\cos\alpha_{opt}} \equiv \frac{(r_2-r_1)^2}{8L\sqrt{r_2r_1}} \cdot \\ &\frac{1}{\sqrt{\left[\frac{\left(\frac{r_2+r_1}{2}\right)^2}{r_2r_1}+1\right]^2-\left(\frac{r_2+r_1}{L}\right)^2}}; \quad |\epsilon|_{max} \sim (18-22)\cdot|\eta'|_{max} \end{aligned}\right\} \qquad (16c)$$

Weighted tracking error as function of radial position

$$\frac{\eta'}{|\eta'|_{max}} = 2\frac{\left(p-\frac{x_m}{x}\right)^2}{p^2-1} - 1 \equiv 2\left[\frac{r_2+r_1-\frac{2r_2r_1}{r}}{r_2-r_1}\right]^2 - 1. \qquad (16d)$$

$$\left.\begin{aligned} |\eta'| = |\eta'|_{max} \text{ at } r = r_1, r = r_2, \text{ and } r_0 &= \frac{2r_2r_1}{r_2+r_1} \\ \eta' = 0 \text{ at } r &= \frac{2r_2r_1}{\left(1\mp\frac{1}{\sqrt{2}}\right)r_2+\left(1\pm\frac{1}{\sqrt{2}}\right)r_1} \end{aligned}\right\} \qquad (16e)$$

Fig. 8 shows $\eta'/|\eta'|_{max}$ *vs.* r/r_m, again for the three values $a = 2, 3$, and 4. Comparison of the Figs. 7 and 8 with 6 shows that the two classes of curves correspond, in their character, to the first two Tchebychev polynomials T_1 and T_2. With the values of r_1 and r_2 used previously, it follows then

$$|\epsilon|_{max}\ (\%) \doteq \begin{cases} \dfrac{3.7}{\sqrt{(L_{(inches)})^2 - (5.3)^2}} & (transcription) \\ \dfrac{5.5}{\sqrt{(L_{(inches)})^2 - (3.4)^2}} & (commercial) \end{cases} \qquad (16f)$$

This shows that with an accordingly designed offset arm, it is possible to obtain practically distortion-free tracking even with arms of the shortest practicable length, which is somewhat more than the disk radius.

This result is important as it implies a considerable flexibility of pick-up design, which is necessary in order to meet a number of practical requirements which so far have not been taken into account. One of these factors is the limited accuracy of mounting under practical conditions of production and service. This affects only one of the two parameters, namely, the overhang. It is necessary that the maximum distortion occurring within the playing range does not exceed the prescribed limit as long as the deviation from the optimal overhang *16b* is kept within reasonable tolerances. Another practical factor which has not been considered so far, is connected with the tangential friction force of the stylus in the groove. This gives rise to certain adverse conditions discussed below which depend on the offset angle and are improved by decreasing it from its optimal value *16a*. Finally, multi-purpose tone arms must be designed on a compromise-optimal basis for playing commercial as well as transcription records. This implies deviations from optimal single-purpose design and thus an increase of the maximal distortion. The result *16f* shows that with the theoretical optimal design, tracking distortion is still considerably below the permissible limit even for the shortest practicable arm lengths. Thus it can be expected that sufficient margin is left for taking into account the three factors just mentioned by compromise design not requiring increased arm length, which is undesirable for economic reasons. For straight arms, on the other hand, this is indeed the only means to meet the situation, as seen from *15c* and *15f*. This flexibility of the two-parameter design demonstrates the superiority of the offset head.

It is now necessary to investigate the influence of the stylus friction as well as the general dependence of the maximum distortion on α and δ on the basis of *14*.

(*d*) *The Influence of Stylus Friction.*—Only part of the friction force F between groove and stylus is taken up by the tone arm as this can freely rotate about the axis A (Fig. 5). The remaining component $F_h = F \tan \gamma$ is taken up by the groove wall (Fig. 5). Evidently, γ, and therefore F_h, increases with the offset angle, and for near-optimal offset, F_h is centripetal throughout the play range. This gives rise to an undesirable excess pressure on the inner groove wall which may increase the linear translation loss and create even-order distortion components due to asymmetry of wall deformation.[5] Because of the groove wall inclination, F_h creates a vertical component F_v, which is directed upward. For light-weight pick-ups for high-fidelity reproduction,[21, 22] where the bearing weight is kept to a minimum sufficient to overcome the vertical components of tracking and tracing forces—particularly due to pinch-effect[23, 24]—and spurious accelerations due to unevenness of the record and ambient mechanical vibrations, the influence of the additional force F_v is sometimes considered so detrimental that return to the straight arm is advocated.

A fair estimate of F_v can be obtained for soft records where stylus pressure is most critical. Measurements of the friction for cellulose nitrate show that, from about 10 grams up to a "critical" bearing weight P of 25–30 grams where record wear sets in, F increases linearly with P, according to the empirical relation

$$F \doteq 3 + \frac{P}{4} \quad (F \text{ and } P \text{ in grams}) \qquad (17a)$$

(Ref. 21, Fig. 8, p. 215.) F_h is resolved into three components, *i. e.*, one normal to the groove wall, one tangential (frictional), and the vertical, F_v. For a groove angle of 90 degrees, $F_v = F_h(1 - \rho)/(1 + \rho)$, where ρ denotes the coefficient of friction between groove wall and stylus. $\gamma = \alpha + \eta$. It will be shown below that η attains its largest positive value at the outer radius for any design with $\alpha \leqslant \alpha_{opt}$ (*16a*) and optimal overhang. This gives

$$(F_v)_{max} \doteq \left(3 + \frac{P}{4}\right) \frac{1 - \rho}{1 + \rho} \cdot \tan (\alpha + \eta_2) \quad \text{(grams)}$$

It will be shown that under practical conditions $(\alpha + \eta_2)$ will never exceed 30 degrees appreciably, while ρ will not be smaller than $^1/_4$, the value of the corresponding coefficient in *17a*. With these assumptions,

$$(F_v)_{max} \doteq (1.8 + 0.15P) \cdot \tan(\alpha + \eta_2) \lesssim \frac{12 + P}{11.5} \text{ (grams)}. \quad (17b)$$

(For offset angles $\alpha \geqslant \alpha_{opt}$, it will be found that $|\eta|_{max}$ is small compared with α; then tan α may be substituted in *17b*.) For a bearing weight of 15 grams—approximately the lowest commercially available—equation *17b* gives $(F_v)_{max} = 1^1/_2$ and $2^1/_3$ grams for $\alpha + \eta_2 = 20°$ and 30°, respectively; for the "critical" weight of 30 grams, 2.3 grams and 3.6 grams, respectively. Considering these values, it must be borne in mind that only the difference between tan η_2 for the straight arm and tan$(\alpha + \eta_2)$ for the offset arm represents the increase of F_v due to offsetting. As η_2 is much larger for $\alpha = 0$ than for $\alpha = \alpha_{opt}$, this increase of F_v is considerably smaller than F_v itself, usually one-half or less of the values found, as will be shown by numerical examples. It appears therefore that even for the lowest bearing weights commercially used, the increase of F_v due to offsetting is inconsiderable, and that there is certainly no reason for giving up the offset with its inherent advantages on that account. However, a choice of α somewhat $< \alpha_{opt}$ (*16a*) will give some benefit without exceeding the permissible distortion.

(*e*) *Compromise Design and Influence of Mounting Error.*—It has been shown that for practical reasons, it is partly desirable, partly unavoidable to deviate from the theoretical optimal design values *16*. In order to see how far one can go in this respect without infringement on the distortion limit set, the dependence of distortion on α and δ according to *14* must be investigated. For this purpose, it is useful to introduce the numerical radius

$$x_0 = \frac{-2\delta - \delta^2}{\sin \alpha} \quad (18)$$

where η' attains its minimum η'_0. In terms of x_0 and sin α, it is

$$\eta' = \frac{x_m}{2 \cos \alpha} \left\{ 1 - \frac{\sin \alpha}{x} \left(2 - \frac{x_0}{x} \right) \right\} \quad (18a)$$

Starting from $\alpha = 0$, let us first increase the offset continually under adjustment of the underhang or overhang δ for Tchebychev approximation. Between $\alpha = 0$ where $\delta > 0$, and $\alpha = \alpha_{opt}$ where $\delta < 0$, there must be an angle α_0 for which $\delta = 0$, *i. e.*, where the stylus tip passes through the center C (Fig. 5). It follows

$$\sin \alpha_0 = \frac{x_m}{2p} \equiv \frac{x_2 x_1}{x_2 + x_1} \equiv \frac{r_2 r_1}{L(r_2 + r_1)}; \quad \delta(\alpha_0) = 0. \quad (19)$$

This angle is convenient from the point of ease of mounting. For α_0, the radius x_0 (*18*) becomes zero; it is negative, *i. e.*, has no significance, for $\alpha < \alpha_0$. For α_0, x_0 is thus still outside the playing range $x_1 \leqslant x \leqslant x_2$, which implies that the $\eta'(x)$ is monotonic increasing over the playing range, like the curves of Fig. 7. With further increase of α, however, x_0 becomes $= x_1$. Then the curve $\eta'(x)$ has a horizontal tangent at $x = x_1$. The corresponding value of α is called α_{crit}, and it follows

$$\sin \alpha_{crit} = \frac{x_1}{1 - \frac{1}{2}\left(1 - \frac{x_1}{x_2}\right)^2} \equiv \frac{r_1}{L\left[1 - \frac{1}{2}\left(1 - \frac{r_1}{r_2}\right)\right]^2} \qquad (20)$$

For $\alpha > \alpha_{crit}$, the curve $\eta'(x)$ has a negative slope at $x = x_1$ up to the

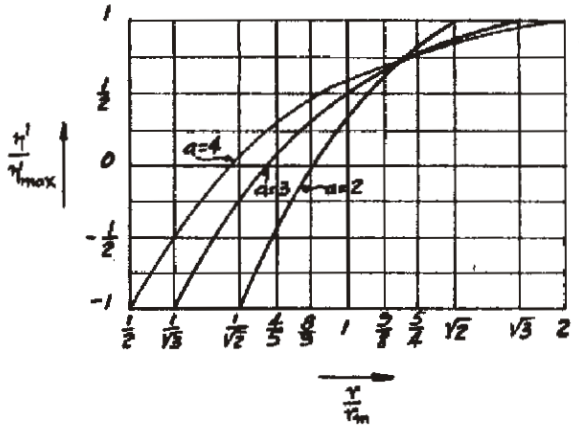

FIG. 7. Relative weighted tracking error *vs.* relative groove radius for straight arms.

minimum at $x = x_0$; then it increases again to η'_2. Tchebychev's approximation is then obtained by making $|\eta'_0| = |\eta'_2| \equiv |\eta'|_{max}$, and not by $|\eta'_1| = |\eta'_2|$, which would give a higher value of $|\eta'|_{max}$. (This is readily shown and follows also from continuity with the domain $\alpha < \alpha_{crit}$.) The value η'_1, which in this range of values of α does not play any part in the Tchebychev design, lies between $\eta'_0 = -\eta'_{max}$ and $\eta'_2 = +\eta'_{max}$ and increases, with increasing α, monotonically from $-\eta'_{max}$ at $\alpha = \alpha_{crit}$ to $+\eta'_{max}$ for $\alpha = \alpha_{opt}$ (eq. *16a*). This case, which has already been dealt with in equation *16* and Fig. 8, represents the second-order approximation. Increasing α beyond α_{opt} leads into the domain where $-\eta'_0 = \eta'_1 = |\eta'|_{max}$ and $\eta'_2 < \eta'_1$. Finally,

there should be an upper critical value of α where η'_2 has decreased to $-\eta'_0$, and x_0 has increased to x_2. For this offset angle,

$$\sin \alpha = \frac{x_2}{1 - \frac{1}{2}\left(\left(\frac{x_2}{x_1}\right)^2 - 1\right)}. \qquad (20a)$$

For practical values of x_1 and x_2, this leads to imaginary α, *i. e.*, under actual conditions, $x_0 < x_2$ for α up to 90°.

The design formulas for different offsets follow.

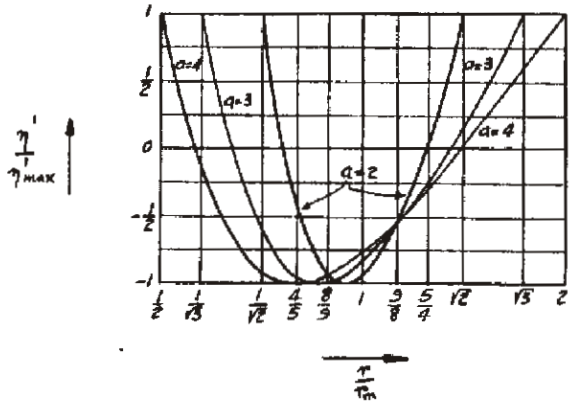

FIG. 8. Relative weighted tracking error *vs.* relative groove radius for offset arms.

For $\alpha \leqslant \alpha_{crit}$, we obtain:

$$\left.\begin{aligned} -\eta'_1 = \eta'_2 = |\eta'|_{max} &= \frac{(x_2 - x_1)\sqrt{x_2 x_1}}{(x_2^2 + x_1^2)\cos\alpha}\left\{\frac{x_2 + x_1}{2} - \sin\alpha\right\} \\ \frac{\eta'}{|\eta'|_{max}} &= \frac{\left(\frac{x_2}{x}\right)^2(x - x_1)(x + x_1 - 2\sin\alpha) - \left(\frac{x_1}{x}\right)^2(x_2 - x)(x_2 + x - 2\sin\alpha)}{(x_2 - x_1)(x_2 + x_1 - 2\sin\alpha)} \\ -2\delta - \delta^2 &= 2\,\frac{(x_1^{-1} + x_2^{-1})\sin\alpha - 1}{x_1^{-2} + x_2^{-2}};\ \delta = 0 \text{ for } \sin\alpha_0 = \frac{1}{x_1^{-1} + x_2^{-1}} \end{aligned}\right\} \qquad (21)$$

For $\alpha = 0$, this reduces, of course, to equation *15*. For $\alpha_{crit} \leqslant \alpha \leqslant \alpha_{opt}$:

$$\left.\begin{aligned} -\eta'_0 = \eta'_2 = |\eta'|_{max} &= \frac{1}{2\cos\alpha}\sqrt{\frac{x_1}{x_2}}\left\{\sqrt{\sin^2\alpha + (x_2 - \sin\alpha)^2} - \sin\alpha\right\} \\ \frac{\eta'}{|\eta'|_{max}} &= \frac{x_2\left\{1 - \frac{2\sin\alpha}{x} + \left[\sqrt{\sin^2\alpha + (x_2 - \sin\alpha)^2} - (x_2 + \sin\alpha)\right]\cdot\frac{x_2}{x^2}\right\}}{\sqrt{\sin^2\alpha + (x_2 - \sin\alpha)^2} - \sin\alpha} \\ x_0 &= \frac{x_2}{\sin\alpha}\left\{\sqrt{\sin^2\alpha + (x_2 - \sin\alpha)^2} - (x_2 - \sin\alpha)\right\};\ -2\delta - \delta^2 = x_0\sin\alpha \end{aligned}\right\} \qquad (22)$$

For $\alpha \geqslant \alpha_{opt}$:

$$\left.\begin{aligned} \eta'_1 = -\eta'_0 = |\eta'|_{max} &= \frac{1}{2\cos\alpha}\sqrt{\frac{x_2}{x_1}}\left\{\sqrt{\sin^2\alpha + (\sin\alpha - x_1)^2} - \sin\alpha\right\} \\ \frac{\eta'}{|\eta'|_{max}} &= \frac{x_1\left\{1 - \frac{2\sin\alpha}{x} + \left[\sqrt{\sin^2\alpha + (\sin\alpha - x_1)^2} + (\sin\alpha - x_1)\right]\frac{x_1}{x^2}\right\}}{\sqrt{\sin^2\alpha + (\sin\alpha - x_1)^2} - \sin\alpha} \\ x_0 &= \frac{x_1}{\sin\alpha}\left\{\sqrt{\sin^2\alpha + (\sin\alpha - x_1)^2} + (\sin\alpha - x_1)\right\}; -2\delta - \delta^2 = x_0\sin\alpha \end{aligned}\right\} \quad (23)$$

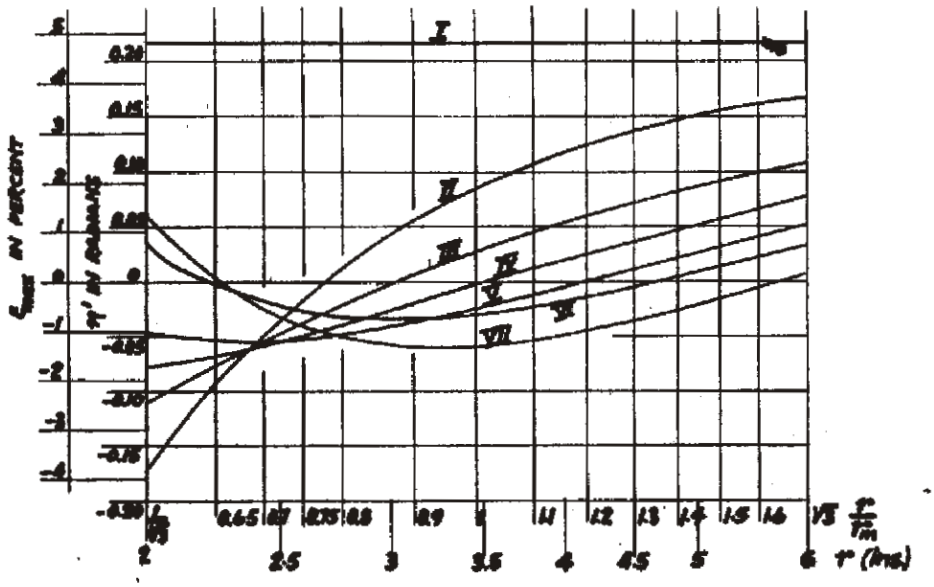

FIG. 9. Numerical example: Plots of weighted tracking error and distortion of optimally hung arm *vs.* groove radius for various offset angles.

Conditions are illustrated in Fig. 9 which shows plots of weighted tracking error and associated harmonic distortion for 2-mil elongation at 500 cps *vs.* the groove radius, for an 8-inch arm and 12-inch disks, with $r_1 = 2$ inches, $r_2 = 6$ inches. The straight line *I* refers to the case of zero offset and underhang, which gives, according to eq. *14*, $\eta' = x_m/2 = 0.217$ rad. $= 12.4°$ or 4.8 per cent distortion, according to *12*. Curve *II* represents $\eta'(x)$ for $\alpha = 0$ and optimal underhang $\delta \doteq {}^9/_{160}$; $d \doteq 0.45$ inch, according to eq. *15*, resulting in $|\eta'|_{max} = 0.173$ rad. $= 9.9°$; the curve is the same as in Fig. 7 for $a = 3$, with different scales. The angle α_0 where $\delta_{opt} = 0$, becomes $\sin\alpha_0 = {}^3/_{16}$, $\alpha_0 = 10.8°$, according to eq. *19;* the associated $\eta'(x)$ with $|\eta'|_{max} = 0.11$ rad. $= 6.4_3°$ is plotted as curve *III;* it leads to

$\gamma_2 = \alpha + \eta_2 = 22°$, which is only $4^1/_2°$ larger than for $\alpha = 0$. Curve *IV* belongs to an angle α which is still <, but close to, α_{crit} and > α_0: $\sin \alpha = {}^2/_7$, $\alpha = 16.6°$; $|\eta'|_{max} = 4.4_4°$; $\alpha + \eta_2 = 24.3°$. According to eq. *20*, $\sin \alpha_{crit} = {}^9/_{28}$, $\alpha_{crit} = 18.7_5°$. Curve *V* refers to $\sin \alpha = {}^5/_{14}$, $\alpha = 20.9°$ which is > α_{crit}. As different from *IV*, the minimum occurs no longer at $x = x_1$, but at $x_0 = 0.290$, according to equation *22*; $-\eta'_1/|\eta'|_{max} = -0.863$; $|\eta'|_{max} = 0.0538$ rad. $= 3.08°$; $\alpha + \eta_2 = 26.2°$. The curve *VI*, the same as in Fig. 8 for $a = 3$, represents the second-order Tchebychev approximation, with $\sin \alpha_{opt}$

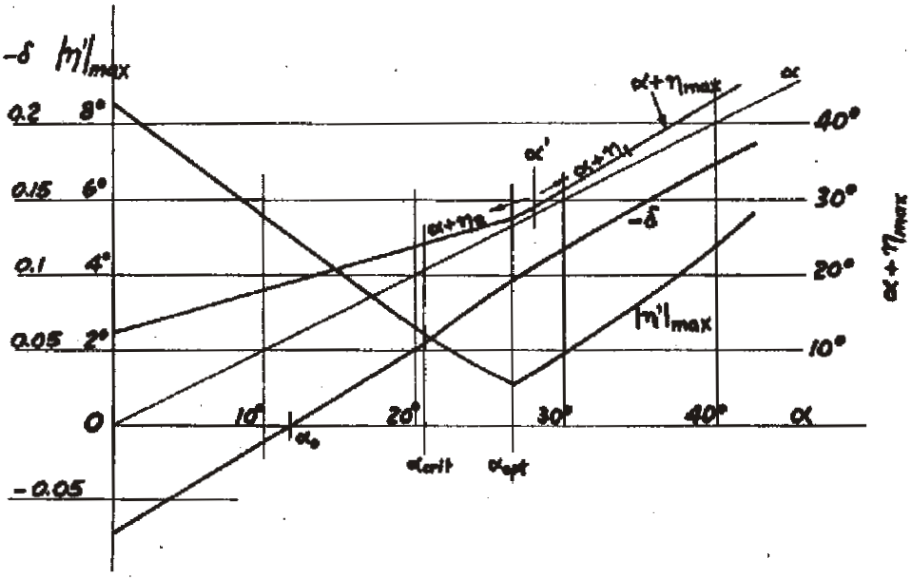

FIG. 10. Numerical example: Plots of various parameters *vs.* offset angle.

$= {}^3/_7$, $\alpha_{opt} = 25^1/_3°$, $x_0 = {}^3/_8$; $|\eta'|_{max} = 0.0343$ rad. $= 1.97°$. The improvement over the straight arm, curve *II*, is striking. $\alpha_{opt} + \eta_2(\alpha_{opt}) = 28^3/_4°$. Finally, curve *VII* pertains to $\sin \alpha = {}^1/_2$, $\alpha = 30° > \alpha_{opt}$, with $\eta'_2 < -\eta'_0 = |\eta'|_{max} = 0.059$ rad. $= 3.38°$; $x_0 = 0.405$; $\eta'_2/|\eta'|_{max} = {}^1/_9$, according to eq. *23*. It is seen that the increase of x_0 and decrease of $\eta'_2/|\eta'|_{max}$ is comparatively slow above α_{opt}, in accordance with the fact that the critical angle (eq. *20a*) is usually non-existent; in the present example, $x_1 = {}^1/_2$, $\eta'_2/|\eta'|_{max} = -{}^7/_9$ for $\alpha = \pi/2$, according to eq. *23*.

Fig. 10 shows the dependence of the optimal numerical underhang or overhang, of the associated maximum weighted tracking error, and of the angle $(\alpha + \eta_{max})$ which occurs in *17b*, on the offset angle α.

The curves refer to 16-inch disks and $33^1/_3$ rpm, with $L = 12$ inches, $r_1 = 3.6$ inches, $r_2 = 8$ inches ($x_1 = 0.3$, $x_2 = {}^2/_3$). The characteristic angles are $\alpha_0 = 12°$, $\alpha_{crit} = 20.7°$, and $\alpha_{opt} = 26.5°$. The kinks of the curves at $\alpha = \alpha_{opt}$ are due to the Tchebychev condition. The minimum of $|\eta'|_{max}$ represents, according to *12*, a maximum distortion of only $^1/_3$ per cent, while about $2^1/_2$ per cent is obtained for the straight arm, which is somewhat more than the permissible limit. It is seen that α may be chosen considerably below α_{opt}, without infringement on the distortion limit, but that the resulting reduction of the vertical force *17b* is comparatively modest, because $(\alpha + \eta_2)$ increases only slowly with α for $\alpha < \alpha_{opt}$. If $\alpha > \alpha_{opt}$, η'_2 becomes rapidly $< \eta'_1$ (curve *VII* of Fig. 9), and for a certain angle α', η_2 becomes $= \eta_1$; for $\alpha > \alpha'$, $\eta_{max} = \eta_1$. According to eq. *23*, it is

$$\left.\begin{aligned} &\sin\alpha' = x_2\left[\sqrt{2\left(1+\frac{x_1}{x_2}\right)}-1\right] \quad (\eta_1 = \eta_2) \\ &\text{and} \\ &\eta_{max} \doteq \eta_1 = \frac{1}{2}\tan\alpha\left[\sqrt{1+\left(1-\frac{x_1}{\sin\alpha}\right)^2}-1\right] \text{ for } \alpha \geqslant \alpha' \end{aligned}\right\} \qquad (24)$$

Thus the curve $(\alpha + \eta_{max})$ has 2 kinks: at $\alpha = \alpha_{opt}$ and $\alpha = \alpha'$. The line α is shown for comparison; it is seen that for $\alpha \geqslant \alpha_{opt}$, $\eta_{max} \ll \alpha$, as expected for $\eta_{max} = \eta_1$. Therefore α may be used instead of $\alpha + \eta_{max} = \gamma_{max}$ in the estimate *17b*.

In order to obtain the influence of inaccurate mounting on tracking distortion, it is necessary to supplement the preceding calculations which concerned the case of optimal overhang $-\delta$ for variable offset angle, by those for variable δ. It has already been mentioned in connection with the straight arm design that distortion increases rapidly if the underhang is increased beyond the optimal value, while a decrease is much less harmful; it can be shown that the ratio of the two effects is $(r_2/r_1)^2$. This is easily understood on the ground that the design is based on the *weighted* tracking error. Conditions are therefore most critical at the inner groove radius. This is true not only for straight arms but for all under-critical offset angles. An illustration is given by Fig. 11, which shows $|\eta'|_{max}$ *versus* $-\delta$ for the same numerical example as used in Fig. 10. The curves are plotted for the four cases $\alpha = 0$, $\alpha = \alpha_0$, $\alpha = \alpha_{crit}$, and $\alpha = \alpha_{opt}$. The unsymmetry noted for $\alpha = 0$ persists up to α_{crit}, while the mounting becomes more and more critical with increasing offset angle due to the

decrease of $|\eta'|_{max}(\delta_{opt})$. For $\alpha > \alpha_{crit}$, the steepness of ascent for $\delta < \delta_{opt}$ increases rapidly, due to the appearance of the minimum η_0. At $\alpha = \alpha_{opt}$, the inclination on the side of positive $(\delta - \delta_{opt})$ is still substantially unaltered, but the side of negative $(\delta - \delta_{opt})$ is now the steeper one. At the same time, the influence of the mounting becomes most severe, which is understood, as the optimal approximation is achieved through compensation. In the present numerical example, a deviation $|\delta - \delta_{opt}|$ of about 4.10^{-3} corresponding to a mounting error of only $^3/_{64}$ inch, already doubles the value of $|\eta'|_{max}$. The full realization of the second-order approximation would thus call for an accuracy of a few tenths of a millimeter. But as the dis-

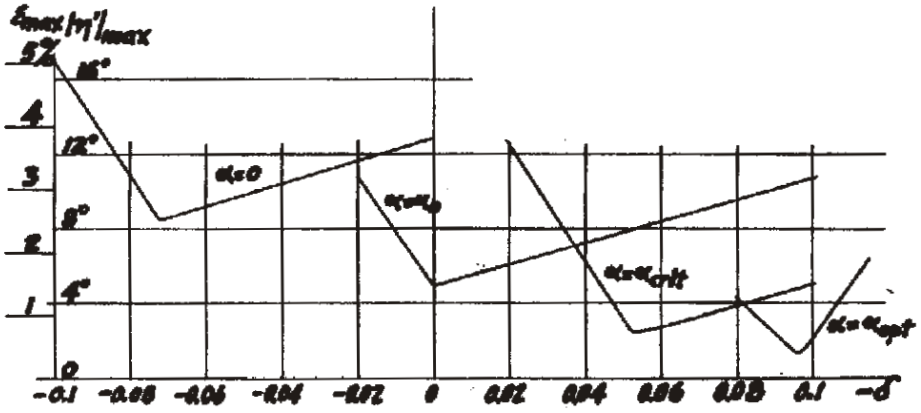

FIG. 11. Numerical example: Distortion *vs.* mounting error for characteristic offset angles.

tortion associated with the minimum of $|\eta'|_{max}$ is far below the permissible limit, requirements can be considerably relaxed, under practical conditions. Liberal mounting tolerances of about $^1/_2$ to 1 per cent of the arm length or $\pm^1/_{16}$ to $^1/_8$ inch will be permissible in most practical cases. They are easily determined by calculating the slopes of the $|\epsilon|_{max}$–δ curves at both sides of $\delta = \delta_{opt}$ (α). For all designs with $\alpha < \alpha_{opt}$, which were found preferable on account of the decrease of F_y (*17*), an overhang δ somewhat larger than δ_{opt} should be prescribed, which is likewise found in terms of the two slopes.

(*f*) *Design of Multi-Purpose Arms.*—When it is desired to play records of different sizes and/or speeds with the same tone arm, this should be designed on a compromise basis so as to render as small as possible the maximal tracking distortion occurring under any conditions thus included. As the mean radii r_m of different types of disk

records are different, the design is based on the original relations *10* and *14* or *18a* combined:

$$\epsilon \doteq \frac{v}{2L\Omega \cos \alpha}\left(1 - \frac{\sin \alpha}{x}\left(2 - \frac{x_0}{x}\right)\right); \quad x_0 = \frac{-2\delta - \delta^2}{\sin \alpha} \qquad (25)$$

It should furnish for α and x_0 such values that minimize $|\epsilon|_{max}$ simultaneously for the different types of records which are characterized by their values of Ω, r_1, and r_2, v being considered as constant (*i. e.*, 8 cm/sec at 500 cps for permissible $|\epsilon|_{max} = 2$ per cent). In practice, only the following combinations are used

(*1*) 78 rpm; $r_1 \sim 2$ inches, $r_2 \sim 6$ inches
(*2*) 78 rpm; $r_1 \sim 2$ inches, $r_2 \sim 8$ inches
(*3*) $33^1/_3$ rpm; $r_1 \sim 3^1/_3$ inches, $r_2 \sim 8$ inches

For design purposes, (*1*) can be disregarded as it is fully included in the range of (*2*). Using upscripts in referring to (*2*) and (*3*), the following six values have to be considered as potential maxima of distortion

$$\Delta_1^{(2)} = \left|1 - \frac{\sin \alpha}{x_1^{(2)}}\left(2 - \frac{x_0}{x_1^{(2)}}\right)\right|; \quad \Delta_0^{(2)} = \left|1 - \frac{\sin \alpha}{x_0}\right|; \quad \Delta_2^{(2)} = \left|1 - \frac{\sin \alpha}{x_2^{(2)}}\left(2 - \frac{x_0}{x_2^{(2)}}\right)\right|;$$

$$\Delta_1^{(3)} = 2.34\left|1 - \frac{\sin \alpha}{x_1^{(3)}}\left(2 - \frac{x_0}{x_1^{(3)}}\right)\right|; \quad \Delta_0^{(3)} = 2.34\left|1 - \frac{\sin \alpha}{x_0}\right|;$$

$$\Delta_2^{(3)} = 2.34\left|1 - \frac{\sin \alpha}{x_2^{(3)}}\left(2 - \frac{x_0}{x_2^{(3)}}\right)\right|.$$

Here, Δ stands as abbreviation for $(2L\Omega_2 \cos \alpha)|\epsilon|/v$ with $\Omega_2 = 78\pi/30$ sec^{-1}; 2.34 = ratio of the two speeds. $\Delta_0^{(k)}$ has to be omitted if $x_0^{(k)} \leqslant x_1^{(k)}$ ($k = 2$ or 3) as being outside the playing range. The optimal numerical values of x_0 and sin α are those which minimize the largest of the four to six Δ's, *i. e.*, which make the three largest of them equal. $\Delta_2^{(2)}$ can obviously be omitted from the comparison, but not necessarily $\Delta_0^{(2)}$, as x_0 may be $< x_1^{(3)}$ but $> x_1^{(2)}$.

As an example, the design of a double-purpose 12-inch arm is given. The numerical limit radii are $x_1^{(2)} = {}^1/_6$, $x_1^{(3)} = {}^7/_{24}$, and $x_2^{(2)} = x_2^{(3)} = {}^2/_3$. It is found that for $|\Delta_1^{(2)}| = |\Delta_1^{(3)}| = |\Delta_2^{(3)}| \equiv \Delta_{max}$, $|\Delta_0^{(2)}| < \Delta_{max}$ and $x_1^{(3)} > x_0 = 0.288_5$; sin $\alpha = 0.344$; $\alpha = 20.1°$. $\delta = 0.050_9$, $d = 0.61_1$ inch. Fig. 12 shows the resulting distortion ϵ, according to *25*, for $v = 8$ cm/sec at 500 cps; its maximum is only 1 per cent. This is only half the permissible limit and leaves thus a safety margin for inaccurate mounting. It is seen that x_0 is only slightly $< x_1^{(3)} = 0.292$; *i. e.*, for the speed $33^1/_3$, the design is close to that for $\alpha = \alpha_{crit}$. For the speed 78 rpm, on the other hand, $\alpha > \alpha_{opt}$, and the overhang

$-\delta < -\delta_{opt}(\alpha)$. If the same arm were to be used for 78 rpm alone, the optimal design as given by equation *16* would be: $\alpha_{opt} = 19°$, $-d_{opt} = 0.532$ inch, $|\epsilon|_{max} = 0.39$ per cent; if it were designed for use at $33^1/_3$ rpm alone: $\alpha_{opt} = 26°$, $-d_{opt} = 1.023$ inches, $|\epsilon|_{max} = 0.36$ per cent. It is seen that the double-purpose design lies closer to the first case.

OTHER EFFECTS OF TRACKING ERROR

The harmonic distortions due to tracking error depend, as shown, only on the distortion parameter ϵ (*4a*), *i. e.*, on the weighted tracking error η' (*11*). Consequently, the design was based on this quantity.

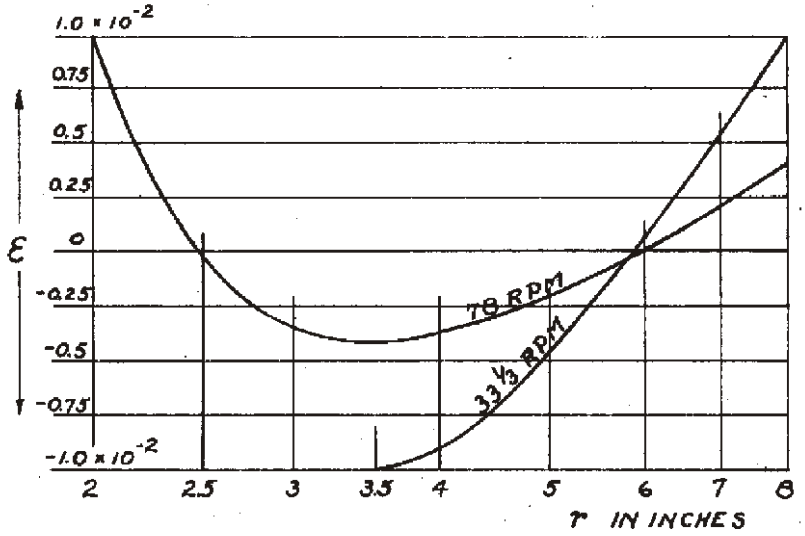

FIG. 12. Numerical example for multi-purpose arm design: Tracking distortion over playing range.

There are, however, effects which depend on the tracking error η itself rather than on η'. Although they are in general unimportant, they should at least be mentioned here.

Going back to the rigorous expressions *6*, *7*, and *8* for the picked-up signal, it is seen that this contains the factor sec η. This implies an increase, not only in signal amplitude, but also in the lateral reaction force (both stiffness and inertia), by sec η. This increase, however, is of negligible magnitude for all practical purposes although the design minimizing $|\eta'|_{max}$ does not minimize $|\eta|_{max}$. The largest value which η may take occurs at the outer rim for straight arms. It was shown (Part II, *b*) that even for maximal permissible distortion—

which is nearly obtained with a properly underhung 8-inch arm for 12-inch records— $\eta_2 \doteq 18°$, *i. e.* $(\sec \eta_2 - 1) \doteq 0.05 \ll 1$. This is in line with the assumption $\eta^2/2 \ll 1$ on which the design procedure was based.

It has been claimed that tracking error may cause appreciable record wear. Again, this supposed wear would not depend on η' and therefore would not be minimized by the proposed design. But, as in case of the signal amplitude, it does not seem that, within the permissible range as based on the presented design method, tracking error could have any noticeable effect of this kind. No clear experimental evidence of additional record wear caused by tracking error of usual magnitude has ever been presented. Careful listening tests undertaken by Olney[2] did not reveal any clear effect. Besides, it is hard to understand how record wear could ever be produced by tracking error of permissible magnitude. For permanent stylus points, it is certainly ruled out as they are surfaces of revolution. All commercial light-weight pick-ups have permanent styli. In case of steel needles, on the other hand, high stylus tip pressure and motional impedance cause appreciable record wear, quite independently of the tracking mechanism. Wear due to tracking error is supposedly caused by the rate of change of tracking error along the groove spiral: the needle is initially ground to fit the groove and is therefore no longer a surface of revolution; turning about its axis due to change of η therefore entails regrinding of the projecting edge. It is certainly hard to see how this regrinding which occurs very gradually as compared with the initial grinding in the first few grooves, could possibly cause any wear noticeable against the background of that due to excessive stylus pressure and impedance, as met in cheaper grade pick-ups.

I wish to tender my acknowledgment to the Brush Development Company for making this work possible. I am also obliged to Dr. S. J. Begun, head of the recording department, for hints and enlightening discussions.

REFERENCES

[1] MACDONALD, G. E.: "The Reduction of Pick-Up Tracking Error," *Communications*, **XXI** (Jan., 1941), p. 55.

[2] OLNEY, B.: "Phonograph Pick-Up Tracking Error *vs.* Distortion and Record Wear," *Electronics*, X (Nov., 1937), p. 19.

[3] LÖFGREN, E. G.: "On the Non-Linear Distortion in the Reproduction of

Phonograph Records Caused by Angular Deviation of the Pick-Up Arm," *Akust. Zeits.*, III (1938), p. 350.

[4] LEWIS, W. D., AND HUNT, F. V.: "A Theory of Tracing Distortion in Sound Reproduction from Phonograph Records," *J. Acoust. Soc. Amer.*, XII (Jan., 1941), p. 348.

[5] KORNEI, O.: "On the Playback Loss in the Reproduction of Phonograph Records," *J. Soc. Mot. Pict. Eng.*, XXXVII (Dec., 1941), p. 569. After completion of the manuscript, a paper by G. Guttwein, *Akust. Zeits.*, V (Dec., 1940), p. 330, on linear and non-linear distortions in recording and playback, was received.

[6] FELDTKELLER, R., AND WOLMAN, W.: "Almost-Linear Networks," *Telegraph. u. Fernsprech. Tech.*, XX (1931), p. 167.

[7] BARTLETT, A. C.: "Calculation of Modulation Products," *Phil. Mag.*, Part I, XVI (Oct., 1933), p. 834; Part II, XVII (Mar., 1934), p. 628.

[8] LAGRANGE, J. L.: *Hist. de l'Acad. R. des Sci. de Berlin*, XXV (1771), p. 242.

[9] BESSEL, F. W.: *Berliner Abh.* (1826).

[10] WATSON, G. N.: "A Treatise on the Theory of Bessel Functions," Cambridge (1922).

[11] MCLACHLAN, N. W.: "Bessel Functions for Engineers," Part I, Oxford (1934).

[12] JAHNKE-EMDE: "Tables of Functions," Third Ed., Leipsic and Berlin (1938), p. 147.

[13] LAGRANGE, J. L.: *Mem. de l'Acad. de Berlin XXIV*, Oeuvres, II, p. 25.

[14] WHITTAKER, E. T., AND WATSON, G. N.: "A Course of Modern Analysis," Fourth Ed., Cambridge (1935), 7:31 and 7:32, p. 131.

[15] MASSA, F.: "Permissible Amplitude Distortion of Speech in an Audio Reproducing System," *Proc. IRE*, XXI (May, 1933), p. 682.

[16] LYNCH, T. E., AND BEGUN, S. J.: "General Considerations of the Crystal Cutter," *Communications*, XX (Dec., 1940), p. 9.

[17] TCHEBYCHEV, P. L.: *Mem. Acad. Sc. Petersb.*, Series 6, VII (1859), p. 199; Oeuvres, I, p. 271.

[18] GUILLEMIN, E. A.: "Communication Networks," II (1935), p. 386.

[19] CAUER, W.: "An Interpolation Problem with Functions with Positive Real Values," *Math. Zeits.*, XXXVIII (1933), p. 1.

[20] COURANT, R., AND HILBERT, D.: "Methods of Mathematical Physics," Berlin, I (1931), p. 75.

[21] WILLIAMS, A. L.: "Further Improvements in Lightweight Record Reproducers and Theoretical Considerations Entering into Their Design," *J. Soc. Mot. Pict. Eng.*, XXX (Aug., 1939), p. 203.

[22] LYNCH, T. E.: "Some Considerations in Phonograph Pick-Up Design," *Brush Strokes*, III (April–June, 1939), p. 3.

[23] PIERCE, J. A., AND HUNT, F. V.: "Distortion in Sound Reproduction from Phonograph Records," *J. Soc. Mot. Pict. Eng.*, XXXI (Aug., 1938), p. 157; *J. Acoust. Soc. Amer.*, X (July, 1938), p. 14.

[24] FLEMING, L.: Notes on Phonograph Pick-Ups for Lateral-Cut Records," *J. Acoust. Soc. Amer.*, XII (Jan., 1941), p. 366.